# Nucleon strangeness form factors from $N_f = 2 + 1$ clover fermion lattice QCD

Takumi Doi,[1,*] Mridupawan Deka,[1] Shao-Jing Dong,[1] Terrence Draper,[1]
Keh-Fei Liu,[1] Devdatta Mankame,[1] Nilmani Mathur,[2] and Thomas Streuer[3]
($\chi$QCD Collaboration)

[1] *Department of Physics and Astronomy, University of Kentucky, Lexington KY 40506, USA*
[2] *Department of Theoretical Physics, Tata Institute of Fundamental Research, Mumbai 40005, India*
[3] *Institute for Theoretical Physics, University of Regensburg, 93040 Regensburg, Germany*

We present the $N_f = 2+1$ clover fermion lattice QCD calculation of the nucleon strangeness form factors. We evaluate disconnected insertions using the Z(4) stochastic method, along with unbiased subtractions from the hopping parameter expansion. We find that increasing the number of nucleon sources for each configuration improves the signal significantly. We obtain $G_M^s(0) = -0.017(25)(07)$, where the first error is statistical, and the second is the uncertainties in $Q^2$ and chiral extrapolations. This is consistent with experimental values, and has an order of magnitude smaller error.

PACS numbers: 13.40.-f, 12.38.Gc, 14.20.Dh



## I. INTRODUCTION

The structure of the nucleon plays an essential role in understanding the dynamics of QCD, and experiments have been providing many intriguing and unexpected results for decades. In particular, the strangeness content of the nucleon attracts a great deal of interest lately. As the lightest non-valence quark structure, it is an ideal probe for the virtual sea quarks in the nucleon. Extensive experimental/theoretical studies indicate that the strangeness content varies significantly depending on the quantum number carried by the $s\bar{s}$ pair: the scalar density is about 10–20% of that of up, down quarks, the quark spin is $-10$ to 0% of the nucleon, and the momentum fraction is only a few percent of the nucleon. Recently, intensive experiments have been carried out for the electromagnetic form factors by SAMPLE [1], A4 [2], HAPPEX [3], and G0 [4], through parity-violating electron scattering (PVES). The global analyses [5, 6, 7] have produced, e.g., $G_E^s(Q^2) = -0.008(16)$ and $G_M^s(Q^2) = 0.29(21)$ at $Q^2 = 0.1\text{GeV}^2$ [6], but substantial errors still exist so that the results are consistent with zero. Making tighter constraints on these form factors from the theoretical side is one of the challenges in QCD calculation. Moreover, such constraints, together with experimental inputs, can lead to more precise determinations of various interesting quantities, such as the axial form factor $G_A^s$ [7], and the electroweak radiative corrections including the nucleon anapole moment, $\tilde{G}_A$ [5, 8].

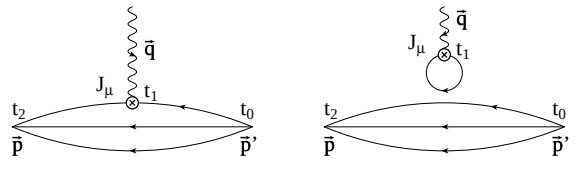


FIG. 1: Two different representations for the 3pt function.

Unfortunately, the theoretical status of strangeness form factors remains quite uncertain. For instance, the values for the magnetic moment $G_M^s(0)$ from different analyses vary widely: $-0.31(9)$ in the dispersion relation (DR) with pole ansatz [9], $-(0.15-0.51)$ in DR with scattering kaon clouds [10], 0.035 in the quark model [11], and $0.08 - 0.13$ in the chiral quark-soliton model [12]. The analyses for the electric form factor are similarly ambiguous. Under these circumstances, the most desirable study is the first-principle calculation in QCD, such as the lattice simulation. However, the calculation requires the evaluation of the disconnected insertion (DI) (Fig. 1 (right)), which is much more difficult compared to the connected insertion (CI) (Fig. 1 (left)) calculation, because the straightforward calculation of DI requires all-to-all propagators, and is prohibitively expensive. Consequently, there are only few DI calculations, where the all-to-all propagators are stochastically estimated. The first calculation was done in the quenched approximation with Wilson fermion [13] and gave $G_M^s(0) = -0.36(20)$, and $-0.28(10)$ from the updated calculation [14]. Another quenched DI calculation with Wilson fermion [15] obtained $G_M^s(0.1\text{GeV}^2) = 0.05(6)$. There are also several indirect estimates using quenched [16, 17] or unquenched [18] lattice data for the CI part, and the experimental magnetic moments (or electric charge radii) for octet baryons as inputs under the assumption of isospin symmetry. These estimates obtained $G_M^s(0) = -0.046(19)$ [16] and $G_M^s(0) = -0.066(26)$ [18].

In this paper, we provide the first full QCD lattice simulation of the direct DI calculation with high statistics. The paper is organized as follows. In Sec. II, the formulation and parameter setup of the lattice calculation are presented. Technical details to improve the DI eval-

*Electronic address: doi@pa.uky.edu;
Present Address: Graduate School of Pure and Applied Science, University of Tsukuba, Tennodai 1-1-1, Tsukuba, Ibaraki 305-8571, Japan.

TABLE I: The setup parameters as well as hadron masses. $N_{noise}$ is the number of noises in the stochastic estimate and $N_{src}$ is the number of nucleon sources for each configuration.

| $\kappa_{ud}$ | $N_{conf}$ | $N_{noise}$ | $N_{src}$ | $m_\pi a$ | $m_K a$ | $m_N a$ |
|---|---|---|---|---|---|---|
| 0.13760 | 800 | 600 | 64 | 0.5141(5) | 0.5141(5) | 1.0859(12) |
| 0.13800 | 810 | 600 | 82 | 0.4302(6) | 0.4540(5) | 0.9623(16) |
| 0.13825 | 810 | 800 | 82 | 0.3717(7) | 0.4141(6) | 0.8844(20) |

uation are also given. In Sec. III, we present the lattice QCD data, and carefully examine the possible systematic uncertainties. Sec. IV is devoted to the summary of our results.

## II. FORMALISM

We employ $N_f = 2+1$ dynamical configurations with nonperturbatively $\mathcal{O}(a)$ improved clover fermion and RG-improved gauge action generated by CP-PACS/JLQCD Collaborations [19]. We use $\beta = 1.83$ and $c_{sw} = 1.7610$ configurations with the lattice size of $L^3 \times T = 16^3 \times 32$. The lattice spacing was determined using $K$-input or $\phi$-input [19]. We use the averaged scale of $a^{-1} = 1.625$GeV hereafter, as the uncertainty of the scale is negligible compared to the statistical error in our results. For the hopping parameters of $u$,$d$ quarks ($\kappa_{ud}$) and $s$ quark ($\kappa_s$), we use $\kappa_{ud} = 0.13825$, 0.13800, and 0.13760, which correspond to $m_\pi = 0.60$, 0.70, and 0.84 GeV, respectively, and $\kappa_s = 0.13760$ is fixed. We perform the calculation only at the dynamical quark mass points, with the periodic boundary condition in all directions.

We calculate the three point function (3pt) $\Pi^{\rm 3pt}_{J_\mu}$ and two point function (2pt) $\Pi^{\rm 2pt}$ defined as

$$\Pi^{\rm 3pt}_{J_\mu}(\vec{p},t_2;\ \vec{q},t_1;\ \vec{p'}=\vec{p}-\vec{q},t_0) = \sum_{\vec{x}_2,\vec{x}_1} e^{-i\vec{p}\cdot(\vec{x}_2-\vec{x}_0)}\times e^{+i\vec{q}\cdot(\vec{x}_1-\vec{x}_0)}\langle 0|{\rm T}\left[\chi_N(\vec{x}_2,t_2)J_\mu(\vec{x}_1,t_1)\bar{\chi}_N(\vec{x}_0,t_0)\right]|0\rangle \quad (1)$$

$$\Pi^{\rm 2pt}(\vec{p},t;\ t_0) = \sum_{\vec{x}} e^{-i\vec{p}\cdot(\vec{x}-\vec{x}_0)}\langle 0|{\rm T}\left[\chi_N(\vec{x},t)\bar{\chi}_N(\vec{x}_0,t_0)\right]|0\rangle, \quad (2)$$

where $\chi_N = \epsilon_{abc}(u_a^T C\gamma_5 d_b)u_c$ is the nucleon interpolation field and the insertion $J_\mu$ is given by the point-split conserved current $J_\mu(x+\mu/2) = (1/2)\times\left[\bar{s}(x+\mu)(1+\gamma_\mu)U^\dagger_\mu(x)s(x) - \bar{s}(x)(1-\gamma_\mu)U_\mu(x)s(x+\mu)\right]$.

Electromagnetic form factors can be obtained using $\vec{p}=\vec{0}$, $\vec{p'}=-\vec{q}$ kinematics for the forward propagation ($t_2 \gg t_1 \gg t_0$) [13]. In this work, we consider the backward propagation ($t_2 \ll t_1 \ll t_0$) as well, in order to increase statistics. The formulas for Sachs electric (magnetic) form factors $G^s_E$ ($G^s_M$) are summarized as

$$R^\pm_\mu(\Gamma^\pm_{\rm pol}) \equiv \frac{{\rm Tr}\left[\Gamma^\pm_{\rm pol}\cdot\Pi^{\rm 3pt}_{J_\mu}(\vec{0},t_2;\ \pm\vec{q},t_1;\ -\vec{q},t_0)\right]}{{\rm Tr}\left[\Gamma^\pm_e\cdot\Pi^{\rm 2pt}(\pm\vec{q},t_1;\ t_0)\right]} \times \frac{{\rm Tr}\left[\Gamma^\pm_e\cdot\Pi^{\rm 2pt}(\vec{0},t_1;\ t_0)\right]}{{\rm Tr}\left[\Gamma^\pm_e\cdot\Pi^{\rm 2pt}(\vec{0},t_2;\ t_0)\right]}, \quad (3)$$

$$R^\pm_{\mu=4}(\Gamma^\pm_{\rm pol}=\Gamma^\pm_e) = \pm G^s_E(Q^2), \quad (4)$$

$$R^\pm_{\mu=i}(\Gamma^\pm_{\rm pol}=\Gamma^\pm_k) = \frac{\mp\epsilon_{ijk}q_j}{E^q_N+m_N}G^s_M(Q^2), \quad (5)$$

where $\{i,j,k\}\neq 4$, $\Gamma^\pm_e \equiv (1\pm\gamma_4)/2$ , $\Gamma^\pm_k \equiv (\pm i)/2\times(1\pm\gamma_4)\gamma_5\gamma_k$ and $E^q_N \equiv \sqrt{m_N^2+\vec{q}^2}$. The upper (lower) sign corresponds to the forward (backward) propagation.

Furthermore, we consider another kinematics of $\vec{p}=\vec{q}$, $\vec{p'}=\vec{0}$, where the analogs of Eqs. (3), (4), (5) hold. We find that the results from the latter kinematics have similar size of statistical errors as those from the former, and the average of them yields better results. Hereafter, we present results from total average of two kinematics and forward/backward propagations, unless otherwise noted.

The calculations of 3pt functions for the strangeness current need the evaluation of DI. We use the stochastic

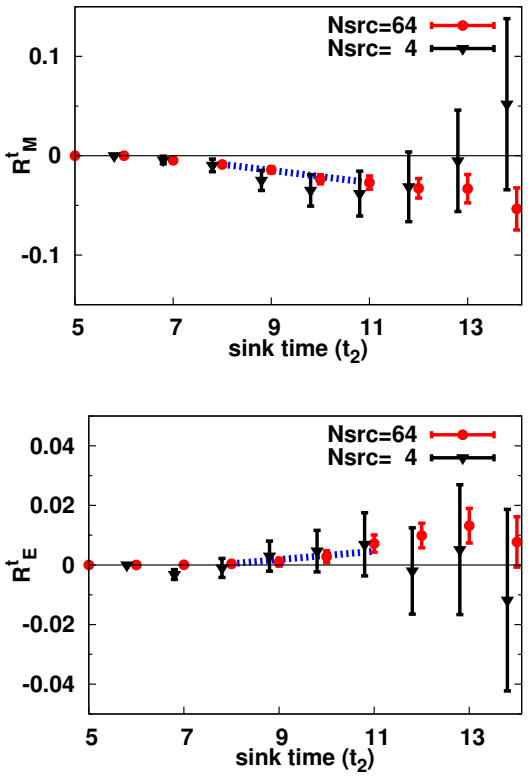


FIG. 2: $R^t_M$ (upper) and $R^t_E$ (lower) with $\kappa_{ud} = 0.13760$, $\vec{q}^2 = 2\cdot(2\pi/La)^2$, $N_{src} = 64$ (circles) and $N_{src} = 4$ (triangles, with offset for visibility), plotted against the nucleon sink time $t_2$. The dashed line is the linear fit where the slope corresponds to the form factor.

TABLE II: Lattice results for the strangeness electromagnetic form factors with the momentum-squared $\vec{q}^2 = n \cdot (2\pi/La)^2$.

| | $G_M^s(Q^2)(\times 10^{-2})$ | | | | $G_E^s(Q^2)(\times 10^{-2})$ | | | | |
|---|---|---|---|---|---|---|---|---|---|
| $\kappa_{ud}\backslash n$ | 1 | 2 | 3 | 4 | 0 | 1 | 2 | 3 | 4 |
| 0.13760 | -0.96(29) | -0.61(17) | -0.57(20) | -0.20(25) | 0.21(21) | 0.01(10) | 0.14(08) | 0.22(11) | 0.10(15) |
| 0.13800 | -0.76(37) | -0.76(24) | -0.57(32) | 0.04(41) | 0.15(28) | 0.16(14) | 0.14(12) | 0.15(19) | 0.46(29) |
| 0.13825 | -1.09(41) | -1.02(27) | -0.67(33) | -0.25(47) | -0.04(33) | -0.16(15) | 0.36(13) | 0.27(20) | 0.71(31) |

TABLE III: The parameters fitted against $Q^2$ behavior.

| | $G_M^s(Q^2)$ | | | $G_E^s(Q^2)$ | |
|---|---|---|---|---|---|
| $\kappa_{ud}$ | $G_M^s(0)$ $(\times 10^{-2})$ | $\Lambda a$ | $\chi^2$/dof | $g_E^s$ $(\times 10^{-2})$ | $\chi^2$/dof |
| 0.13760 | -1.7(12) | 0.66(29) | 0.34(83) | 1.2(5) | 0.56(89) |
| 0.13800 | -1.4(09) | 0.77(40) | 0.77(126) | 1.4(6) | 0.34(70) |
| 0.13825 | -1.9(11) | 0.80(40) | 0.38(87) | 1.9(7) | 2.68(189) |

method [20], with Z(4) noises in color, spin and space-time indices. We generate independent noises for different configurations, in order to avoid possible autocorrelation. To reduce fluctuations, we use the charge conjugation and $\gamma_5$-hermiticity (CH), and parity symmetry. For instance, we find that the information for the $G_M^s$ is coded in the product of $\mathrm{Re}(\Pi^{2\mathrm{pt}}) \times \mathrm{Re}(\mathrm{loop})$, and filtering out the imaginary parts reduces the noises [21, 22]. We also perform unbiased subtractions [23] to reduce the off-diagonal contaminations to the variance. For subtraction operators, we employ those obtained through hopping parameter expansion (HPE) for the propagator $M^{-1}$ [23], $\frac{1}{2\kappa}M^{-1} = \frac{1}{1+C} + \frac{1}{1+C}(\kappa D)\frac{1}{1+C} + \cdots$ where $D$ denotes the Wilson-Dirac operator and $C$ the clover term. We subtract up to order $(\kappa D)^4$ term, and observe that the statistical error is reduced by a factor of 2.

In the stochastic method, it is quite expensive to achieve a good signal to noise ratio (S/N) just by increasing $N_{noise}$ because S/N improves with $\sqrt{N_{noise}}$. In view of this, we use many nucleon point sources $N_{src}$ in the evaluation of the 2pt part for each configuration [22]. Since the calculations of the loop part and 2pt part are independent of each other, this is expected to be an efficient way. In particular, for the $N_{noise} \gg N_{src}$ case, we observe that S/N improves almost ideally, by a factor of $\sqrt{N_{src}}$. We take $N_{src} = 64$ for $\kappa_{ud} = 0.13760$ and $N_{src} = 82$ for $\kappa_{ud} = 0.13800, 0.13825$, where locations of sources are taken so that they are separated in 4D-volume as much as possible. The calculation parameters as well as basic hadron masses are tabulated in Tab. I.

There are several ways [13, 15] to extract the matrix elements from Eqs. (4) and (5) with various $t_1, t_2$ results. Among them, it is advocated [13, 14, 21, 22] to take the summation over the insertion time $t_1$, symbolically given as $R_{E,M}^t \equiv \frac{1}{K_{E,M}^{\pm}} \sum_{t_1=t_0+t_s}^{t_2-t_s} R_\mu^\pm = \text{const.} + t_2 \times G_{E,M}^s$, where $K_{E,M}^{\pm}$ are trivial kinematic factors appearing in Eqs. (4) and (5), and $t_s$ is chosen so that the error is minimal. We thus obtain $G_{E,M}^s$ as the linear slope of $R_{E,M}^t$ against $t_2$. In order to achieve ground state saturation, we use the data only for $t_2 \geq 7$ [22].

## III. RESULTS AND DISCUSSIONS

We calculate for the five smallest momentum-squared points, $\vec{q}^2 = n \cdot (2\pi/La)^2$ $(n = 0\text{–}4)$, which correspond to $|\vec{q}| = 0, 0.64, 0.90, 1.1, 1.3$ GeV. Typical figures for $R_M^t$, $R_E^t$ are shown in Fig. 2. One can observe the significant S/N improvement by increasing $N_{src}$. The numerical results are given in Tab. II. We note $G_E^s(0)$ are consistent with zero, which serves as a test of the calculations. Of particular interest is that, for all $\kappa_{ud}$ simulations, $G_M^s(Q^2)$ is found to be negative with 2-3 $\sigma$ signals for low $Q^2$ regions.

In order to determine the magnetic moment, the $Q^2$ dependence of $G_M^s(Q^2)$ is studied. We employ the dipole form in the $Q^2$ fit, $G_M^s(Q^2) = G_M^s(0)/(1 + Q^2/\Lambda^2)^2$, where reasonable agreement with lattice data is observed. For the electric form factor, we employ $G_E^s(Q^2) = g_E^s \cdot Q^2/(1 + Q^2/\Lambda^2)^2$, considering that $G_E^s(0) = 0$ from the vector current conservation. In the practical fit of $G_E^s(Q^2)$, however, reliable extraction of the pole mass $\Lambda$ is impossible because $G_E^s(Q^2)$ data are almost zero within error. Therefore, we assume that $G_E^s(Q^2)$ has the same pole mass as $G_M^s(Q^2)$, and perform a one-parameter fit for $g_E^s$. The obtained parameters are given in Tab. III. We also test the simultaneous fit of $G_M^s(Q^2)$ and $G_E^s(Q^2)$ with three parameters of $G_M^s(0), \Lambda, g_E^s$, and confirm that the results are consistent with the values in Tab. III.

Finally, we perform the chiral extrapolation for the fitted parameters. Since our quark masses are relatively heavy, we consider only the leading dependence on $m_K$, which is obtained by heavy baryon chiral perturbation theory (HB$\chi$PT). For the magnetic moment $G_M^s(0)$, we fit linearly in terms of $m_K$ [13, 24]. For the pole mass $\Lambda$, we take that the magnetic mean-square radius $\langle r_s^2 \rangle_M \equiv -6\frac{dG_M^s}{dQ^2}|_{Q^2=0} = 12G_M^s(0)/\Lambda^2$ behaves as $1/m_K$ [24]. For $g_E^s$, we use the electric radius $\langle r_s^2 \rangle_E \equiv -6\frac{dG_E^s}{dQ^2}|_{Q^2=0} = -6g_E^s$ which has an $\ln(m_K/\mu)$ behavior [24], and we take the scale $\mu = 1$ GeV. The chiral extrapolated results are $G_M^s(0) = -0.017(25)$, $\Lambda a = 0.58(16)$, $\langle r_s^2 \rangle_M = -7.4(71) \times 10^{-3}\mathrm{fm}^2$ and $g_E^s = 0.027(16)$ (or $\langle r_s^2 \rangle_E = -2.4(15) \times 10^{-3}\mathrm{fm}^2$).

Before quoting the final results, we consider the systematic uncertainties yet to be addressed. First, we analyze the ambiguity of $Q^2$ dependence in form fac-

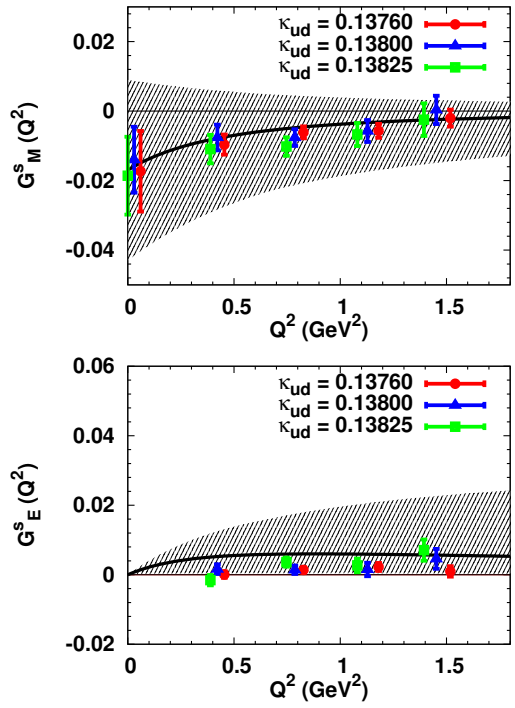


FIG. 3: The chiral extrapolated results for $G_M^s(Q^2)$ (upper) and $G_E^s(Q^2)$ (lower) plotted with solid lines. Shaded regions represent the error-band with statistical and systematic error added in quadrature. Shown together are the lattice data (and $Q^2$-extrapolated $G_M^s(0)$) for $\kappa_{ud} = 0.13760$ (circles), 0.13800 (triangles), 0.13825 (squares) with offset for visibility.

tors, which is rather unknown for the strangeness. We also study the monopole form, $G_M^s(Q^2) = G_M^s(0)/(1 + Q^2/\tilde{\Lambda}^2)$, $G_E^s(Q^2) = g_E^s \cdot Q^2/(1 + Q^2/\tilde{\Lambda}^2)$, and find that the precision of the lattice data cannot disentangle the difference of the dipole/monopole behaviors. The results from the monopole fit are $G_M^s(0) = -0.024(39)$, $\tilde{\Lambda}a = 0.34(17)$, $\langle r_s^2\rangle_M = -12(18)\times 10^{-3}\mathrm{fm}^2$ and $g_E^s = 0.035(17)$ (or $\langle r_s^2\rangle_E = -3.1(15) \times 10^{-3}\mathrm{fm}^2$), which are consistent with those from the dipole fit and have relatively larger statistical errors.

Second, we study the uncertainties in chiral extrapolation by testing two alternative extrapolations. In the first one, we take into account the nucleon mass dependence on the quark mass, using the lattice nucleon mass. From the physical viewpoint, this corresponds to measuring the magnetic moment not in units of lattice magneton but physical magneton [25]. We obtain $G_M^s(0) = -0.017(24)$, $\Lambda a = 0.77(21)$, $\langle r_s^2\rangle_M = -4.6(43) \times 10^{-3}\mathrm{fm}^2$ from the dipole fit, and $G_M^s(0) = -0.023(36)$, $\tilde{\Lambda}a = 0.45(22)$, $\langle r_s^2\rangle_M = -7(11) \times 10^{-3}\mathrm{fm}^2$ from the monopole fit, while $G_E^s$ cannot be fitted because fit dof are not sufficient. Note that results are consistent with previous analyses. In the second alternative, we use the linear fit in terms of $m_K^2$, observing the results have weak quark mass dependence. We obtain $G_M^s(0) = -0.017(21)$, $\langle r_s^2\rangle_M = -3(17) \times 10^{-3}\mathrm{fm}^2$, $g_E^s = 0.023(12)$ (or $\langle r_s^2\rangle_E = -2.0(10) \times 10^{-3}\mathrm{fm}^2$) from the dipole fit, and $G_M^s(0) = -0.023(33)$, $\langle r_s^2\rangle_M = -8(43) \times 10^{-3}\mathrm{fm}^2$, $g_E^s = 0.029(12)$ (or $\langle r_s^2\rangle_E = -2.5(11) \times 10^{-3}\mathrm{fm}^2$) from the monopole fit, while pole masses are found to suffer from too large statistical errors to extract useful information. We find again the results are consistent with previous analyses. While a further clarification with physically light quark mass simulation and a check on convergence of HB$\chi$PT [26] is desirable, we use the dependence of results on different extrapolations as systematic uncertainties in the chiral extrapolation.

Third, we examine the contamination from excited states. Because our spectroscopy study indicates that the mass of Roper resonance is massive compared to the $S_{11}$ state on the current lattice [27], the dominant contaminations are (transition) form factors associated with $S_{11}$. On this point, we find that such contaminations can be eliminated theoretically, by making the following substitutions: $\Gamma_e^{\pm} \to \tilde{\Gamma}_e^{\pm} \equiv (1 \pm m_{N^*}/E_{N^*}^q \cdot \gamma_4)/2$ in Eq. (3), $\{\Gamma_e^{\pm},\ \Gamma_k^{\pm}\} \to \{\tilde{\Gamma}_{\pm}^{p'_-}\Gamma_e^{\pm},\ \tilde{\Gamma}_{\pm}^{p'_-}\Gamma_k^{\pm}\}$ in Eqs. (4) and (5). Here, $m_{N^*}$ denotes the $S_{11}$ mass, $E_{N^*}^q \equiv \sqrt{m_{N^*}^2 + \vec{q}^2}$, $\tilde{\Gamma}_{\pm}^{p'_-} \equiv (m_{N^*} \mp i\not{p}'_-)/(2m_{N^*})$ with $p'_- \equiv (E_{N^*}^{p'_-}, \vec{p}')$. Note also that the (r.h.s.) of Eqs. (4) and (5) have modifications in the kinematical factor, which we do not show explicitly. It is found that the results from these equations are basically the same as before, so we conclude that the contamination regarding the $S_{11}$ state is negligible.

As remaining sources of systematic error, one might worry that the finite volume artifact could be substantial considering that the physical spacial size of the lattice is about $(2\mathrm{fm})^3$. However, we recall that Sachs radii are found to be quite small, $|\langle r_s^2\rangle_{E,M}| \ll 0.1\mathrm{fm}^2$, which indicates a small finite volume artifact. For the discretization error, we first examine the error associated with the finite momentum $\vec{q}$, using the dispersion relation of the nucleon. We find that the nucleon energy at each $\vec{q}$ on the lattice is consistent with the dispersion relation, and conclude that finite $(qa)$ discretization error is negligible. As another discretization error, we note that $m_N$ $(m_K)$ is found to have 6 (8) % error for the current configurations [19, 28]. Considering the dependence of $G_{E,M}^s$ on these masses, we estimate that the discretization errors in our results amount to $\lesssim 10\%$, and are much smaller than the statistical errors. Of course, more quantitative investigations on these issues are necessary with larger and finer lattices, and such work is in progress.

Here, we present our final results. For the magnetic moment, $G_M^s(0) = -0.017(25)(07)$, where the first error is statistical and the second is systematic from uncertainties of the $Q^2$ extrapolation and chiral extrapolation. We also obtain $\Lambda a = 0.58(16)(19)$ for dipole mass or $\tilde{\Lambda}a = 0.34(17)(11)$ for monopole mass, and $g_E^s = 0.027(16)(08)$. These lead to $G_M^s(Q^2) = -0.015(23)$, $G_E^s(Q^2) = 0.0022(19)$ at $Q^2 = 0.1\mathrm{GeV}^2$, where error is

obtained by quadrature from statistical and systematic errors. Note that these are consistent with the world averaged data [5, 6, 7], with an order of magnitude smaller error. In Fig. 3, we plot $G_M^s(Q^2)$, $G_E^s(Q^2)$, where the shaded regions correspond to the square-summed error. The lattice data for each $\kappa_{ud}$ are also plotted.

## IV. SUMMARY

We have studied the strangeness electromagnetic form factors of the nucleon using $N_f = 2 + 1$ clover fermion configurations. In the evaluation of the disconnected insertion (DI), the Z(4) stochastic method along with unbiased subtractions from the hopping parameter expansion has been used. We have developed several techniques to achieve a good S/N in the DI calculation, and found that increasing the number of nucleon sources for each configuration is particularly efficient. For all quark mass simulations, $G_M^s(Q^2)$ has been found to be negative with 2-3 $\sigma$ signals for low $Q^2$ regions. Upon $Q^2$ and chiral extrapolations, we have obtained $G_M^s(Q^2 = 0) = -0.017(25)(07)$, where the first error is statistical, and the second reflects the uncertainties in $Q^2$ and chiral extrapolations. We have also obtained $G_M^s(Q^2) = -0.015(23)$, $G_E^s(Q^2) = 0.0022(19)$ at $Q^2 = 0.1\mathrm{GeV}^2$, where error is obtained by quadrature from statistical and systematic errors. These results are consistent with experimental values, and our errors are an order of magnitude smaller.

### Acknowledgments

We thank the CP-PACS/JLQCD Collaborations for their configurations. This work was supported in part by U.S. DOE grant DE-FG05-84ER40154. Research of N.M. is supported by Ramanujan Fellowship. The calculation was performed at Jefferson Lab, Fermilab and the Univ. of Kentucky, partly using the Chroma Library [29].

[1] D.T. Spayde *et al.* (SAMPLE Collab.), Phys. Lett. B **583**, 79 (2004).
[2] F.E. Maas *et al.* (A4 Collab.), Phys. Rev. Lett. **93**, 022002 (2004); *ibid.*, **94**, 152001 (2005).
[3] K.A. Aniol *et al.* (HAPPEX Collab.), Phys. Rev. Lett. **96**, 022003 (2006); *ibid.*, Phys. Lett. B **635**, 275 (2006); A. Acha *et al.*, Phys. Rev. Lett. **98**, 032301 (2007).
[4] D.S. Armstrong *et al.* (G0 Collab.), Phys. Rev. Lett. **95**, 092001 (2005).
[5] R.D. Young *et al.*, Phys. Rev. Lett. **97**, 102002 (2006); *ibid.*, **99**, 122003 (2007).
[6] J. Liu *et al.*, Phys. Rev. C **76**, 025202 (2007).
[7] S.F. Pate *et al.*, Phys. Rev. C **78**, 015207 (2008).
[8] M.J. Ramsey-Musolf, nucl-th/0302049 (2003).
[9] R.L. Jaffe, Phys. Lett. B **229**, 275 (1989).
[10] H.-W. Hammer and M.J. Ramsey-Musolf, Phys. Rev. C **60**, 045204 (1999); *ibid.*, 045205 (1999).
[11] P. Geiger and N. Isgur, Phys. Rev. D **55**, 299 (1997).
[12] A. Silva *et al.*, Phys. Rev. D **74**, 054011 (2006).
[13] S.-J. Dong *et al.*, Phys. Rev. D **58**, 074504 (1998).
[14] N. Mathur and S.-J. Dong, Nucl. Phys. Proc. Suppl. **94**, 311 (2001); *ibid.*, **119**, 401 (2003).
[15] R. Lewis *et al.*, Phys. Rev. D **67**, 013003 (2003).
[16] D.B. Leinweber *et al.*, Phys. Rev. Lett. **94**, 212001 (2005); *ibid.*, **97**, 022001 (2006).
[17] P. Wang *et al.*, arXiv:0807.0944 (2008).
[18] H.-W. Lin, arXiv:0707.3844 (2007).
[19] T. Ishikawa *et al.*, PoS (LAT2006), 181 (2006); T. Ishikawa *et al.*, Phys. Rev. D **78**, 011502(R) (2008).
[20] S.-J. Dong and K.-F. Liu, Phys. Lett. B **328**, 130 (1994).
[21] N. Mathur *et al.*, Phys. Rev. D **62**, 114504 (2000).
[22] M. Deka *et al.*, Phys. Rev. D **79**, 094502 (2009).
[23] C. Thron *et al.*, Phys. Rev. D **57**, 1642 (1998).
[24] T.R. Hemmert *et al.*, Phys. Lett. B **437**, 184 (1998); *ibid.*, Phys. Rev. C **60**, 045501 (1999).
[25] M. Göckeler *et al.*, Phys. Rev. D **71**, 034508 (2005).
[26] H.-W. Hammer *et al.*, Phys. Lett. B **562**, 208 (2003).
[27] X. Meng *et al.* ($\chi$QCD Collab.), *in preparation.*
[28] CP-PACS/JLQCD Collab., *private communication.*
[29] R.G. Edwards and B. Joó, Nucl. Phys. Proc. Suppl. **140**, 832 (2005); C. McClendon, `http://www.jlab.org/~edwards/qcdapi/reports/dslash_p4.pdf`